



Article

Intelligent Micro-Cogeneration Systems for Residential Grids: A Sustainable Solution for Efficient Energy Management

Daniel Cardoso ^{1,2} , Daniel Nunes ², João Faria ^{1,3}, Paulo Fael ^{1,2} and Pedro D. Gaspar ^{1,2,*} 

¹ Department of Electromechanical Engineering, Faculty of Engineering, University of Beira Interior, Rua Marquês d'Ávila e Bolama, 6201-001 Covilhã, Portugal; silva.cardoso@ubi.pt (D.C.); joao.pedro.faria@ubi.pt (J.F.); pfael@ubi.pt (P.F.)

² C-MAST-Centre for Mechanical and Aerospace Science and Technologies, 6201-001 Covilhã, Portugal; figueira.nunes@ubi.pt

³ Instituto de Telecomunicações, Universidade da Beira Interior, 6201-001 Covilhã, Portugal

* Correspondence: dinis@ubi.pt

Abstract: This paper presents an optimization approach for Micro-cogeneration systems with internal combustion engines integrated into residential grids, addressing power demand failures caused by intermittent renewable energy sources. The proposed method leverages machine learning techniques, control strategies, and grid data to improve system flexibility and efficiency in meeting electricity and domestic hot water demands. Historical residential grid data were analysed to develop a machine learning-based demand prediction model for electricity and hot water. Thermal energy storage was integrated into the Micro-cogeneration system to enhance flexibility. An optimization model was created, considering efficiency, emissions, and cost while adapting to real-time demand changes. A control strategy was designed for the flexible operation of the Micro-cogeneration system, addressing excess thermal energy storage and resource allocation. The proposed solution's effectiveness was validated through simulations, with results demonstrating the Micro-cogeneration system's ability to efficiently address high electricity and hot water demand periods while mitigating power demand failures from renewable energy sources. The research presents a novel approach with the potential to significantly improve grid resilience, energy efficiency, and renewable energy integration in residential grids, contributing to more sustainable and reliable energy systems.

Keywords: micro-cogeneration systems; internal combustion engines; residential grids; machine learning; control strategies; energy management; grid flexibility; smart grids; electrical energy; thermal energy; renewable energy integration



Citation: Cardoso, D.; Nunes, D.; Faria, J.; Fael, P.; Gaspar, P.D. Intelligent Micro-Cogeneration Systems for Residential Grids: A Sustainable Solution for Efficient Energy Management. *Energies* **2023**, *16*, 5215. <https://doi.org/10.3390/en16135215>

Academic Editor: Holger Hesse

Received: 9 June 2023

Revised: 30 June 2023

Accepted: 4 July 2023

Published: 6 July 2023



Copyright: © 2023 by the authors. Licensee MDPI, Basel, Switzerland. This article is an open access article distributed under the terms and conditions of the Creative Commons Attribution (CC BY) license (<https://creativecommons.org/licenses/by/4.0/>).

1. Introduction

Reliable energy sources are crucial for residential grids, yet renewable solutions like photovoltaic (PV) systems experience irregular power production contingent on resource availability [1]. To address this, this study proposes coupling PV with battery and Micro-cogeneration units as a holistic energy-generation solution. Notably, the incorporation of a Micro-cogeneration system, particularly a Micro combined heat and power (Micro-CHP) system powered by an internal combustion engine, presents a potential pathway towards off-grid residential energy solutions. Micro-cogeneration units are versatile systems producing both electrical and thermal energy. Despite their relatively small size (under 50 kW), they offer opportunities to reduce primary energy consumption and curb greenhouse gas emissions [2–5].

Utilizing the mechanical energy generated by the internal combustion engine converted by an alternator and the thermal energy harvested from the engine's exhaust gases and cooling circuits, these systems can contribute to overall efficiency [6]. Micro-cogeneration presents an opportunity to enhance the stability and resilience of home grids powered by renewable energy sources, thereby overcoming the implementation barrier that

arises from relying solely on renewables. By integrating Micro-cogeneration, home grids can become more energy efficient and resilient. PV panels and battery systems sometimes fall short of consistently meeting the demands of the household grid, particularly during periods of low solar exposure. This current paper proposes that the internal combustion engine in the Micro-CHP system can function as a backup in these instances, supporting electrical demand and charging the batteries while also providing thermal energy for applications such as hot water and space heating. It is intended to analyse and state that the Micro-CHP can support both demands (kW) in integrated grids with PV and battery systems, aiming to keep them off-grid. The challenges associated with implementing this system can be attributed to factors such as the fuel supply network, acquisition costs, maintenance requirements, and adaptation to imposed loads. Overcoming these challenges is crucial for the successful implementation of such a system. This study aims to address these challenges by effectively integrating the electrical production of the Microgeneration system with the imposed load requirements, particularly in the context of photovoltaic energy, where renewable energy production may be limited.

It is important to establish a framework that enables the fulfilling of load requirements imposed on the network while effectively predicting and meeting the thermal demands for domestic hot water and residential heating. To achieve this objective, it aims to employ appropriately sized machines, coupled with prediction networks and energy storage systems. This integrated approach allows for more accurate and efficient management of the system, ultimately mitigating and satisfying the imposed needs. By utilizing advanced prediction technologies and optimizing energy storage, the demands placed on the system can be effectively suppressed, ensuring a reliable and efficient operation. To optimize the operation of the proposed system, machine learning techniques are employed. Specifically, artificial neural networks (ANNs) are used to predict the electrical load and PV power based on the load profile and PV production of the previous day. This innovative approach allows for the proactive planning and control of electrical and thermal energy, enhancing network safety and efficiency. The main challenge, then, is to efficiently interconnect and coordinate these diverse technologies within the network.

The proposed Micro-cogeneration system's performance, integrated with PV panels and batteries, will be analysed using MATLAB simulation.

2. Literature Review

2.1. Micro-Cogeneration Systems with Internal Combustion Engines

Micro-CHP systems featuring internal combustion engines (ICEs) have emerged as the preferred choice for small-scale applications, owing to their robustness and time-tested technology [7]. Nevertheless, regular maintenance is crucial for maintaining their operational viability [8]. These systems demonstrate versatility in terms of fuel use and can be adapted to fulfil the electricity and heat requirements of the infrastructure where they are deployed [9].

The energy yielded from the fuel is apportioned into three parts: approximately one-third is converted into mechanical work, another third dissipates as heat in the exhaust gases, and the remaining third is manifested as internal engine heat losses. Some of these heat losses occur due to various heat transfer mechanisms within the engine's cooling circuit [6].

When implemented into Micro-cogeneration, internal combustion engines generally adopt a standard configuration as depicted in Figure 1. The system's constituent elements comprise an engine, a generator, a heat recovery system—including a water jacket and exhaust gas heat exchangers—and an acoustic isolator. The engine propels the generator through its mechanical energy, while the heat exchangers recover thermal energy from the engine's exhaust system and cooling circuits. A pump typically drives the heat recovery system, prompting the coolant to circulate through the engine and into the heat exchangers, consequently producing hot water [8].

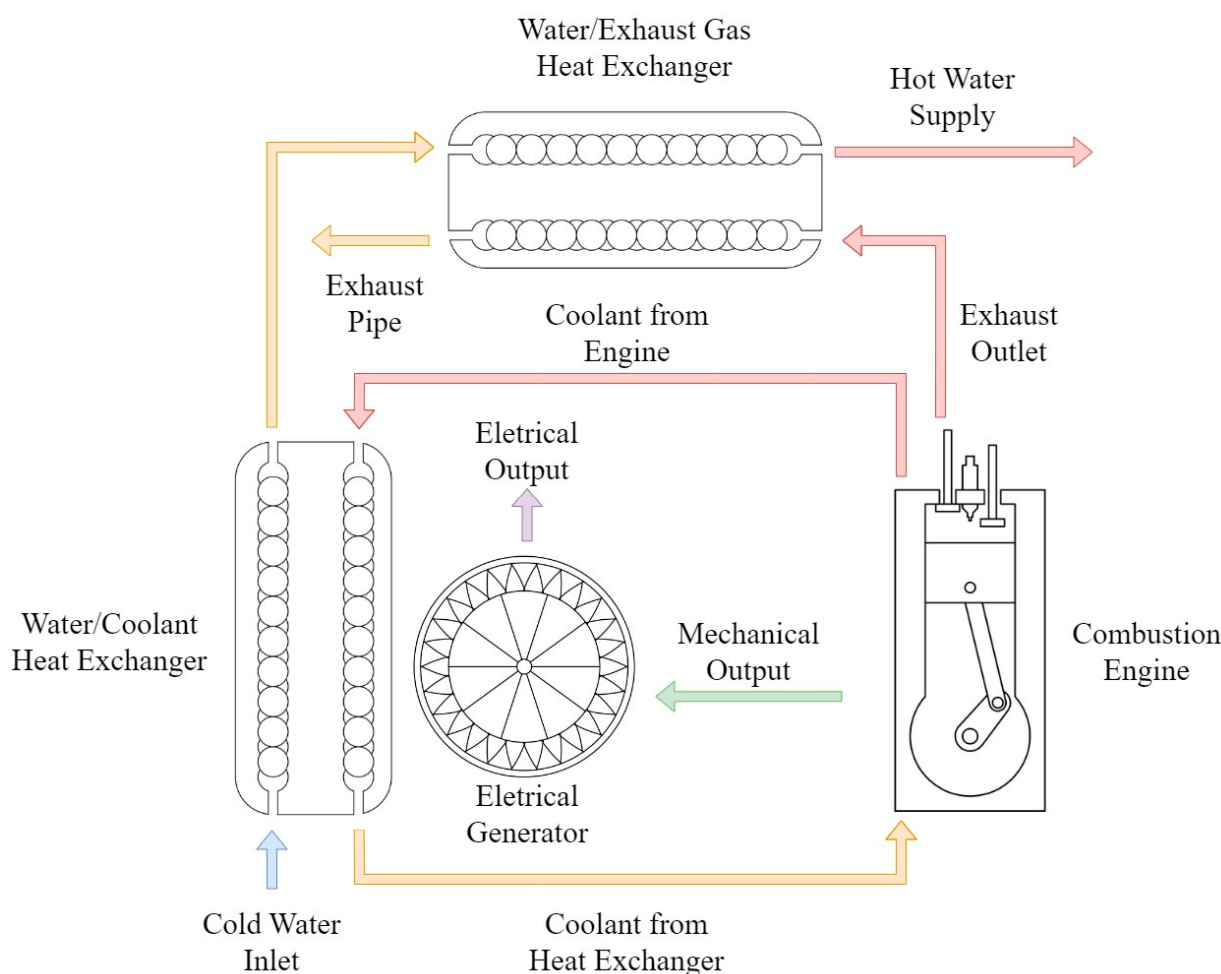


Figure 1. Standard configuration of a Micro-CHP system based on ICE.

Several brands have developed Micro-CHP systems based on internal combustion engines. Honda pioneered the market in 2003 with the Ecovill Micro-CHP unit, selling 100,000 units in Japan [6]. This natural gas-powered unit marked the first Micro-cogeneration system designed with an internal combustion engine, offering 1 kW of electrical power and 3 kW of thermal power with an overall energy efficiency of 85% [10]. An upgraded model launched in 2011 boasted an enhanced overall efficiency of 92% due to the application of the “EXlink” engine, which features an expansion stroke longer than the compression stroke thanks to a multi-link expansion linkage mechanism [11]. Other notable entries into the market include Tokyo Gas’s natural gas-powered 6 kW system with an efficiency of 86% and Yanmar Diesel Engine Co.’s system offering an output of 9.8/8.2 kW, with an efficiency of 81.55% and a heat recovery rate of up to 58/56% [8,12].

In Europe, SenerTec dominates the market, with over 20,000 units sold of their Dachs model, which offers 5.5 kW of electrical power, 10 kW of thermal power, and an overall efficiency of 90% [6,8]. A notable alternative comes from PowerPlus Technologies, which has introduced the Ecopower Micro-CHP unit, providing adjustable electrical power ranging from 4.7 to 1.3 kW thanks to engine rotation control and a frequency converter that conditions the energy output for grid feeding. The unit’s thermal power ranges from 4 to 12.5 kW, with overall efficiency estimated at 89% [6].

2.2. Micro-Cogeneration Systems with Fuel Cells

Fuel cells are devices that produce electrical and thermal energy from chemical energy, without involving combustion cycles. Hydrogen (fuel) and oxygen (oxidant) are the chemical elements used to obtain the two forms of energy. Fuel cells are classified according

to their working temperature or the type of electrolyte. The most suitable for cogeneration systems are alkaline fuel cells (AFCs), proton exchange membranes (PEMs), phosphoric acid fuel cells (PAFCs), molten carbonate fuel cells (MCFCs), and solid oxide fuel cells (SOFCs) [13]. Their use in Micro-cogeneration has advantages such as low emissions, high efficiency, low noise, and greater autonomy, creating independence from the grid [14]. The complex processing or access to hydrogen, the time-consuming start-up, and the complexity of integration in hybrid systems are the main barriers to the introduction of this technology in Micro-cogeneration [15].

2.3. Challenges in Integrating Micro-Cogeneration into Residential Grids

Incorporating an internal combustion engine within the framework of Micro-cogeneration into residential settings with existing photovoltaic panels and batteries poses significant challenges. The primary hurdle is the effective interconnection of all energy systems, aiming to optimize grid profitability while minimizing losses and costs. Consequently, sophisticated and automated control systems are paramount for effective energy management [16].

Darcovich et al. scrutinized a residential grid comprising these technologies and emphasized that utilizing photovoltaic panels and batteries could yield economic benefits, albeit to a lesser extent upon the integration of a Micro-CHP system [17]. The energy consumption hierarchy generally prioritizes photovoltaic power due to its renewable nature, followed by battery usage, and finally, engine operation when the photovoltaic power and battery charge level prove inadequate.

For water heating applications, photovoltaic power is the primary energy source. However, when it falls short, the engine's thermal energy steps in. Compared to conventional water heaters, engines cannot heat water as rapidly, leading to the inclusion of a water cylinder in the system. This component provides a time buffer between the heat produced by the Micro-CHP and the hot water utilized [18].

The complexity arises in deciding where to direct the electrical energy and establishing criteria for using the engine's thermal energy. Further complications could stem from the time taken to charge the battery while the engine simultaneously supports the residence's electrical load. These issues exemplify some of the potential difficulties faced when amalgamating these technologies within a unified grid [17].

2.4. Machine Learning and Control Strategies for Energy Management

Addressing the significant electricity demand from off-grid sources has made energy management a pressing issue in residential settings. Several innovative approaches have emerged, using machine learning and control strategies to manage energy systems effectively, balancing energy distribution, and optimizing the use of photovoltaic panels, batteries, and internal combustion engines in Micro-cogeneration. These strategies strive to decrease energy consumption and enhance overall system performance.

Machine learning models extensively utilized in energy systems include artificial neural networks (ANNs), multilayer perceptron (MLP), extreme learning machine (ELM), support vector machines (SVMs), wavelet neural networks (WNNs), adaptive neuro-fuzzy inference systems (ANFISs), decision trees, deep machine learning, ensemble models, and hybrid advanced machine learning models.

ANNs serve as a framework for various machine learning algorithms designed to process complex data inputs and can be applied to prediction, regression, and curve-fitting methodologies. Their simplicity when faced with multi-variable problems makes them stand out [19]. MLPs are a more sophisticated variant of ANNs, often referred to as feedforward neural networks, widely used in process modelling and prediction [19–21].

An SVM, on the other hand, is particularly suitable for pattern recognition, classification, and regression analysis due to its ability to execute generalizations. Its algorithms, based on statistical learning theory for structural risk minimization, find wide applicability in load forecasting [22].

A WNN leverages a function to process a data series and yield an output value for a specific input value. This model requires less learning time compared to the MLP model [23]. The ANFIS methodology is a fusion of fuzzy logic and neural network features, integrating an ANN based on the Takagi–Sugeno fuzzy inference system, marking it as a hybrid machine learning method [24]. Decision trees utilize a tree-like model to make decisions based on historical electric load data. Deep machine learning employs deep neural networks to predict load based on past data, allowing for more precise future load predictions due to its ability to learn complex, non-linear patterns. Ensemble techniques amalgamate multiple prediction models into an overarching model to enhance prediction accuracy. Finally, hybrid advanced machine learning models combine decision trees and deep neural networks to accomplish highly accurate load forecasting [22].

All the methodologies can be deployed for energy forecasting and control.

3. Data Collection and Analysis

3.1. Residential Grid Data Sources

Load profiles were obtained from the Building America Housing Simulation B10 Benchmark. The base load profile represents the electrical demand (kW) and was estimated by scaling the base load profile from other houses. A random deviation of $\pm 20\%$ was included in the home's load profile to consider variability.

A PV generation profile was collected from the solar radiation database PVGIS-SARAH2, developed to calculate the electricity production of a photovoltaic system as a function of solar radiation and other important climate variables. It is based on data of global horizontal and inclined solar radiation, air temperature, wind speed, and other climatic parameters, provided by meteorological stations or by regional climate models. The model uses simulation and calculation algorithms to estimate the solar radiation of the photovoltaic system, considering values such as latitude, longitude, elevation, declination, azimuth, the nominal power of the PV system, and system losses. The latitude and longitude refer to the location where the data were collected. The parameters and corresponding values used to generate the hourly data in one year are presented in the following table (Table 1).

Table 1. Solar radiation data.

Parameter	Value
Latitude (deg.)	41.157
Longitude (deg.)	−8.391
Elevation (m)	166
Slope (deg.)	37
Azimuth (deg.)	10
Nominal power PV system (kW)	3.5
System losses (%)	15

3.2. Data Analysis and Machine Learning

Artificial neural networks (ANNs) were employed with the generated data to predict the daily load and PV production profiles. These forecasts served as inputs for a controller that determined the operation of the Micro-CHP system and battery. ANNs are advantageous for this application because they can learn from and make predictions based on time-series data. The ANN was trained using 80% of the collected data, with the remaining 20% used for testing. The predicted and actual values were then compared to gauge the performance of the ANN, with the root-mean-square error (RMSE) being used as the performance index. This approach improves the optimized control of the system considering the anticipated load profiles and PV production and thereby enhancing the overall system performance.

4. Mathematical Model

4.1. PV Model

To determine the power output of the photovoltaic modules, a model was used as a function of cell temperature and solar irradiation. The power output of the photovoltaic system (P_{PV}) is given by Equation (1):

$$P_{PV} = \mu_{mppt} \left(P_{STC} \frac{G}{G_{STC}} (1 + \alpha_{VOC} (T_{cell} - T_{STC})) \right) N_s N_p \quad (1)$$

where μ_{mppt} is the efficiency at the maximum power point track (%), P_{STC} is the maximum power under STC (W), G is the given solar irradiance in each time step (Wm^{-2}), G_{STC} is the irradiance under STC (Wm^{-2}), α_{VOC} is the temperature coefficient of the open-circuit voltage under STC ($\text{V } ^\circ\text{C}^{-1}$), T_{STC} is cell temperature under STC conditions ($^\circ\text{C}$), and N_s are the modules connected in series and N_p the modules connected in parallel, in each time step. T_{cell} is the cell temperature in each time step ($^\circ\text{C}$) given by Equation (2):

$$T_{cell} = T_{amb} + \frac{G}{G_{NOCT}} * (\text{NOCT} - T_{NOCT}) \quad (2)$$

With the temperature in each cell given as a function of the ambient temperature T_{amb} in each time step ($^\circ\text{C}$), and G_{NOCT} is the irradiance under NOCT conditions (Wm^{-2}), NOCT is the nominal operating cell temperature ($^\circ\text{C}$), and T_{NOCT} is the air temperature under NOCT conditions ($^\circ\text{C}$) [25,26]. The model specifications are listed in Table 2.

Table 2. PV model specifications.

Parameter	Value
μ_{mppt}	95%
P_{STC}	250 W
G_{STC}	1000 Wm^{-2}
α_{VOC}	$-0.0044 \text{ V } ^\circ\text{C}^{-1}$
T_{STC}	$25 \text{ } ^\circ\text{C}$
G_{NOCT}	800 Wm^{-2}
NOCT	$47.5 \text{ } ^\circ\text{C}$
T_{NOCT}	$20 \text{ } ^\circ\text{C}$

4.2. Battery Model

The kinetic battery model (KiBaM), shown in Figure 2, was proposed by Manwell and McGowan and is used to capture non-linear capacity effects for state-of-charge (SOC) tracking [27].

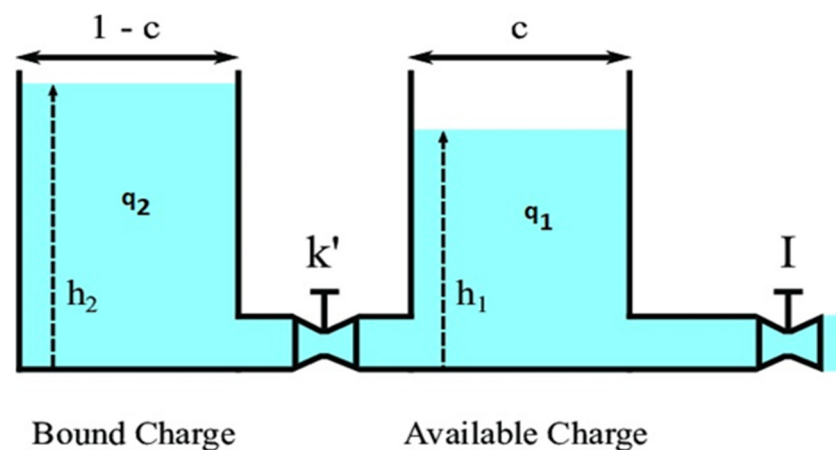


Figure 2. Kinetic battery model (KiBaM) [28].

The KiBaM uses two different reservoirs, called bound charge and available charge, separated by conductance. The available charge reservoir q_1 contains a charge that is immediately available for use by the consumer, and the bound charge reservoir q_2 contains a charge that is chemically bound. Each has the same depth, but different widths and hence different volumes. The width of reservoir 1 (available charge) is c and that of reservoir 2 (bound charge) is $(1 - c)$. The head in each reservoir is given by the width divided by the area.

The battery’s total capacity is the sum of q_1 and q_2 . The variable k represents the rate at which charge flows from q_2 to q_1 [29].

The principle of the KiBaM model is as follows. When the battery is discharging, the charge from q_1 flows out and simultaneously the charge from q_2 flows into q_1 , slowly with k . The charge leaving q_1 is faster than the charge entering, so the height difference between q_1 and q_2 will increase. If the discharge is stopped, the charge from q_2 flows slowly to q_1 until the heights are equal ($h_1 = h_2$), depicted in the battery recovery effect. When the battery is charging, reservoir q_1 charges at a higher rate compared to reservoir q_2 [27]. The amount of energy contained in each reservoir in kWh at each time step is represented by Equations (3) and (4). The kinetic battery model (KiBaM) specifications are listed in Table 3.

$$q'_1 = q_1 e^{-k\Delta t} + \frac{(q_{bat}kc - P_{cd})(1 - e^{-k\Delta t})}{k} - \frac{P_{cd}c(k\Delta t - 1 + e^{-k\Delta t})}{k} \tag{3}$$

$$q'_2 = q_2 e^{-k\Delta t} + q_{bat}(1 - c)(1 - e^{-k\Delta t}) - \frac{P_{cd}(1 - c)(k\Delta t - 1 + e^{-k\Delta t})}{k} \tag{4}$$

Table 3. Kinetic battery model (KiBaM) specifications.

Parameter	Value
k	0.38
c	0.271

In this context, the terms q'_1, q'_2 and q_1, q_2 are the available and bound charge at the beginning and end of each time step, respectively. The variable Δt represents the duration of each time step, while P_{cd} refers to the power used to charge or discharge the system during each time step, measured in kW, given by Equations (5) and (6):

$$P_d = \frac{kq_1 e^{-k\Delta t} + q_{bat}kc(1 - e^{-k\Delta t})}{1 - e^{-k\Delta t} + c(k\Delta t - 1 + e^{-k\Delta t})} \tag{5}$$

$$P_c = \frac{-kcq_{max} + kq_1 e^{-k\Delta t} + q_{bat}kc(1 - e^{-k\Delta t})}{1 - e^{-k\Delta t} + c(k\Delta t - 1 + e^{-k\Delta t})} \tag{6}$$

where q_{max} is the maximum capacity of the battery [29].

4.3. Micro-CHP Model

The Micro-cogeneration system that was chosen for this study was designed to fulfil the specific objectives of the research. It was determined that the system should have an electrical output range between 1.3 and 4.7 kW and a corresponding thermal output ranging from 4 to 12.5 kW. This range was selected to ensure a versatile performance capacity that can adequately respond to the varying demand conditions typically found in residential settings.

To establish the correlation between the electrical and thermal output of the system, a linear equation, Equation (7), was formulated:

$$ICI_T = 2.5 \times ICI_E + 0.75 \tag{7}$$

In Equation (7), ICI_T denotes the thermal power and ICI_E refers to the corresponding electrical power. This relationship implies that for each unit increase in electrical output, the thermal output increases by 2.5 times. The additional constant of 0.75 is the thermal power produced when the electrical output is zero. This formula was developed to provide a simple yet effective way to predict the system's performance across its operating range.

Equation (7) is critical in managing the balance between the electrical and thermal production of the Micro-CHP system. By being able to predict the thermal output for a given electrical output, the system can be operated more efficiently and effectively, ensuring that the heat produced is neither underutilized nor wasted.

In summary, this Micro-CHP model provides a robust framework for understanding and predicting the performance of the system. It serves as a critical tool for optimizing system operation, achieving energy efficiency, and facilitating effective integration with other components of the energy system.

5. Machine Learning-Based Demand Prediction Model

5.1. Model Selection and Rationale

Load forecasting, enabled by machine learning, falls into three primary categories: short-term load forecasting (ranging from one hour to one week), medium-term load forecasting (spanning one week to one year), and long-term load forecasting (extending over a year). Despite the established efficiency of these methods, individual household load forecasting has shown to be more challenging compared to aggregate load forecasting. Two prevalent approaches inform energy forecasting: one based on physical principles and another rooted in statistical methods and machine learning [30].

Artificial neural networks (ANNs), part of the statistical and machine learning approach, simulate the functionality of human brain neurons within a computing framework. In contrast to traditional computing, which excels in storing vast amounts of information and reorganizing it according to specific instructions tailored for that task, ANNs present a novel solution. The potential of ANNs for load prediction has been explored since 1990 [31]. These are parallel networks of simple processing units, designed to emulate the functionalities and structures of the human brain to tackle complex problems [32].

In this study, artificial neural networks have been chosen for the prediction of electrical load and photovoltaic production. Their ability to learn and model non-linear relationships makes them particularly suitable for handling the complexities and fluctuations associated with energy demand and renewable energy production. Their use in this context ensures a more accurate and reliable forecast, which is crucial for efficient energy management and control in residential grids.

5.2. Model Training and Validation

The multi-layer feedforward neural network (FFNN) is one of the most widely used neural networks. In each network layer, each neuron response is provided by the activation function with a cost given by a weighted sum, which acts as a threshold. For any two consecutive layers (input-hidden, hidden-hidden, or hidden-output), $[k - 1, k]$ can be expressed mathematically by Equation (8):

$$y_j = f_j\left(\sum_{i=1}^n \omega_{ij} \times x_i + b_j\right), \quad i \in [0, n] \quad j \in [0, m] \quad (8)$$

where n is the number of neurons in layer $k - 1$ and m is the number of neurons in layer k with $n, m \in \mathbb{Z}^+$; y_j is the output of neuron j , x_i is the input signal to neuron j coming from neuron i ; b_j is the bias of neuron j ; and finally w_{ij} is the synaptic connection weight between neurons i and j [33].

ANN learning is elaborated in a process known as supervised learning, which consists of updating the weight of the vector to minimize the error. In this work, the performance (error) function chosen is the mean squared error, given by Equation (9):

$$MSE = \frac{1}{N} \sum_{i=1}^n (y_i - \hat{y}_i)^2 \quad (9)$$

where N is the number of training samples, \hat{y}_i is the current network output, and y_i is the desired output response [34]. However, when implementing an ANN, a non-trivial set of sensitive aspects, i.e., with an impact on work performance, must be chosen. These aspects include the choice of input variables (load, weather variables, etc.), the size of the training vectors, the number of hidden layers, the number of neurons in each hidden layer, the choice of the training method, the activation functions and the stopping criteria, and a network topology itself [34].

This article employed two feedforward neural networks with a 15-neuron architecture and a single hidden layer to accurately forecast both PV demand and load consumption for the next two hours. These ANNs were designed with five inputs each, specifically chosen to represent lag variables from the training dataset that displayed the strongest correlation. The selection process for these lag variables was conducted through an autocorrelation test, guaranteeing the inclusion of highly influential predictors to enhance the accuracy of the forecasts.

6. Control Strategy for Flexible Operation

Designing the Control Strategy

In the development of the control strategy, energy direction priorities toward different demand types were initially defined. This was necessary to ensure that the resulting simulation would align with the intended requirements. The priority was to ascertain if the photovoltaic production in the upcoming two hours would present a surplus or a deficit when compared to the load forecast for the same duration. The underlying objectives of energy efficiency and economic and environmental sustainability were crucial in the process of optimizing these types of hybrid systems [35]. These considerations were consistently central throughout the development of the strategy.

The simulation operated iteratively for each hour within the following two hours. This resulted in graphical representations of the electric load profile, the water heating profile contained in the electric cylinder, and the state-of-charge (SOC) profile. Current conditions such as SOC, predicted electric load, and forecasted photovoltaic production inform these iterations and align with defined hypotheses.

The selection of a two-hour horizon in the simulation considers several factors to ensure optimal performance of the Micro-cogeneration system. One of the primary considerations is the need to minimize prediction errors in forecasting photovoltaic production and load demand. By limiting the time horizon to two hours, the accuracy of the predictions can be significantly improved, as shorter time intervals generally yield more reliable results. Additionally, the two-hour horizon allows sufficient time for the Micro-cogeneration system to ramp up its energy production to meet the anticipated demand. This is particularly crucial in situations where the system needs to generate thermal energy, as it requires time for the engine to reach optimal operating conditions and produce the desired output. By starting the production of thermal energy within a two-hour timeframe, the Micro-cogeneration system can efficiently answer to the expected demand without compromising its performance. It is important to consider that increasing the time before initiating the production of thermal energy could lead to greater energy losses. This is because the system would need to operate for a longer duration without fulfilling the demand, resulting in wasted energy and reduced overall efficiency. By confining the simulation to a two-hour horizon, the Micro-cogeneration system can align its energy production more closely with the forecasted requirements, minimizing unnecessary energy losses and maximizing energy utilization. In summary, the choice of a two-hour horizon strikes a balance

7. Simulation and Validation

7.1. Simulation Setup and Scenarios (PV/Battery/Micro-CHP)

The residential grid in focus includes an integrated Micro-CHP unit with electrical power ranging from 1.3 to 4.7 kW and thermal power from 4 to 12.5 kW. It has an electrical and thermal efficiency that reaches 24.7% and 64.2%, respectively. The system is also equipped with a battery of 5 kWh capacity and a photovoltaic (PV) panel with a power capacity of 3.5 kWp. It is postulated that the grid is furnished with smart meters that collect and report data for the forthcoming two hours. The data gathered by these smart meters facilitate the intelligent management of the Micro-CHP unit, battery, and PV panel to adequately respond to the electrical demand of the Microgrid. Additionally, the system also manages the demand for hot water stored in a cylinder. This thermal demand can be addressed either by the PV panel, via conversion of excess electrical energy, or directly by the thermal energy produced by the Micro-CHP engine, as depicted in Figure 4.

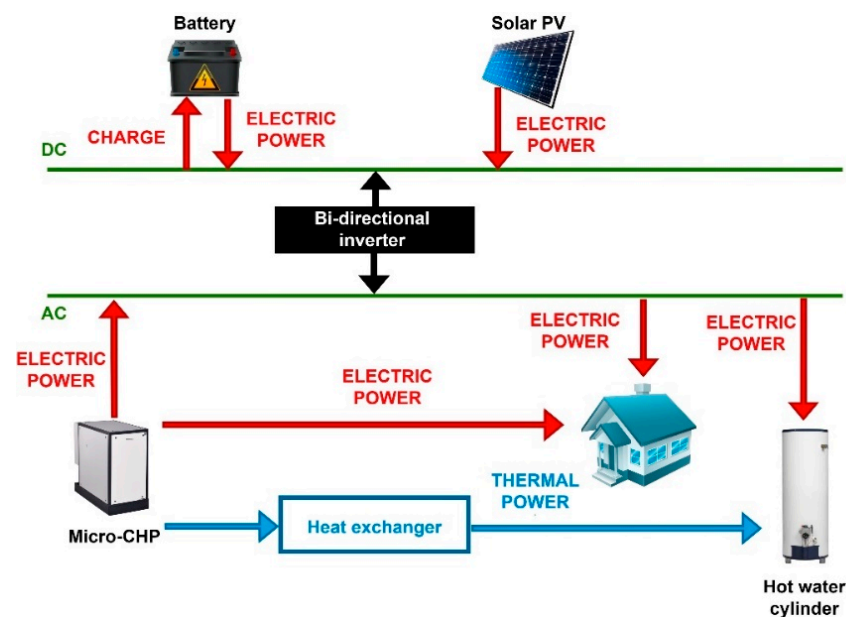


Figure 4. Main components of the simulation.

The forthcoming graphics, based on the simulation run in MATLAB, illustrate different scenarios depending on whether there is an excess or deficit of photovoltaic production, in conjunction with the state of charge (SOC) of the battery. More precisely, scenarios of photovoltaic excess or deficit combined with a low or high SOC will be exhibited at various times throughout the year. These scenarios will be constructed on the prediction of the electric load and photovoltaic production for the forthcoming two hours, utilizing neural network models. These conditions will be put to the test for different combinations of systems, specifically the PV/battery/Micro-CHP, PV/Micro-CHP, and battery/Micro-CHP configurations. The integration of the fuel cell in the system as well as its use for the simulation did not occur due to the usual unavailability of piped hydrogen within a household, compared to natural gas which is much more accessible.

In a load profile comprising 8760 h, an hour was selected for simulation purposes. The SOC of the battery was set for this same hour, and the predictions for the electric load and photovoltaic production for the next two hours were generated using a feedforward neural network. Below are two figures representing the load profile and production profile days. These figures provide a comprehensive view of a 24 h day, with predictions made at 2 h intervals. Figure 5a shows the results for a cloudy day, showcasing the fluctuations in load demand and energy production throughout the day under overcast weather conditions. Conversely, Figure 5b depicts a sunny day, highlighting the load profile and energy production when solar irradiation is abundant.

Consider the case of the system equipped with PV panels, battery, and Micro-CHP. The simulation was conducted for a period where either a deficit or an excess of PV production arises, and the SOC was either lower or higher than 0.2. At 11 am on a cloudy day, for peak demand and a situation where there is a deficit in photovoltaic production and the SOC is less than 0.2, the results are shown in Figure 6.

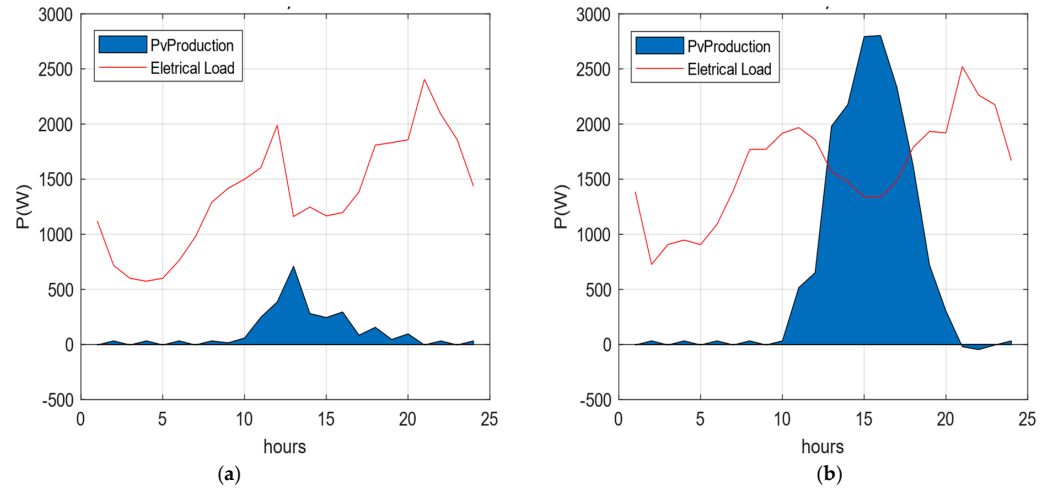


Figure 5. Load profile and production profile days: (a) the scenario of deficit PV production; (b) scenario of excess PV production.

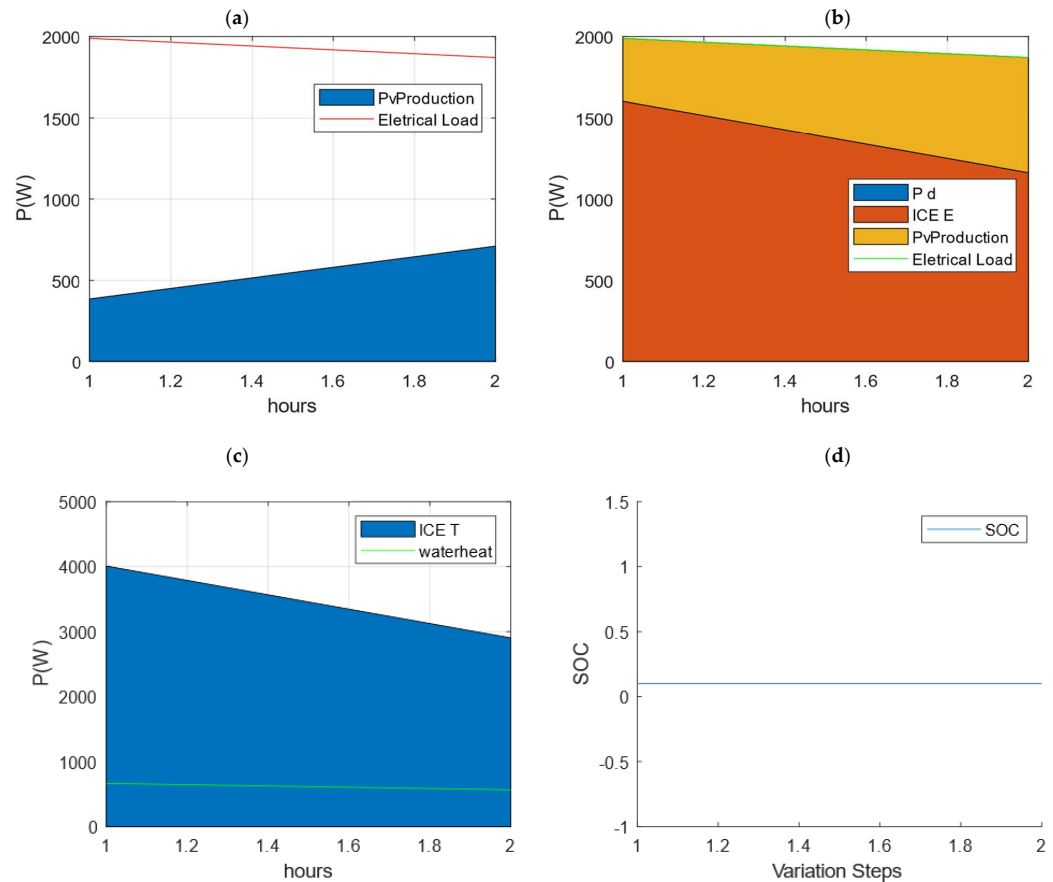


Figure 6. PV production deficit and SOC < 0.2: (a) demand of the electrical load and photovoltaic production; (b) electrical load profile; (c) water heating profile; (d) state of charge during the two prediction hours.

As evident in Figure 6a,b, during the first forecasted hour, the photovoltaic generation deficit (with a projected electrical demand of 1989 W and a photovoltaic power of 386 W) is compensated by 1603 W of electrical energy (ICE E) from the Micro-CHP. Furthermore, 4009 W of thermal energy (ICE T) from the Micro-CHP offsets the demand of 663 W for water heating (as shown in Figure 5c), with 3346 W of thermal surplus being used for storage in a thermal accumulator, from which can be drawn heat for space heating. In the second forecast hour, 1161 W of the electrical power of the engine compensates for the PV production deficit, with a forecasted electric demand of 1871 W and a PV power of 710 W. Given the need to meet the water heating demand, the Micro-cogeneration system compensates the 565 W of demand with 2904 W of thermal power. Here, 2339 W of the thermal surplus is for storage in a thermal accumulator. In Figure 6d, the SOC is kept constant.

In the identical situation of a PV generation deficit, but where the SOC is greater than 0.2, the results for the previous case are shown in Figure 7.

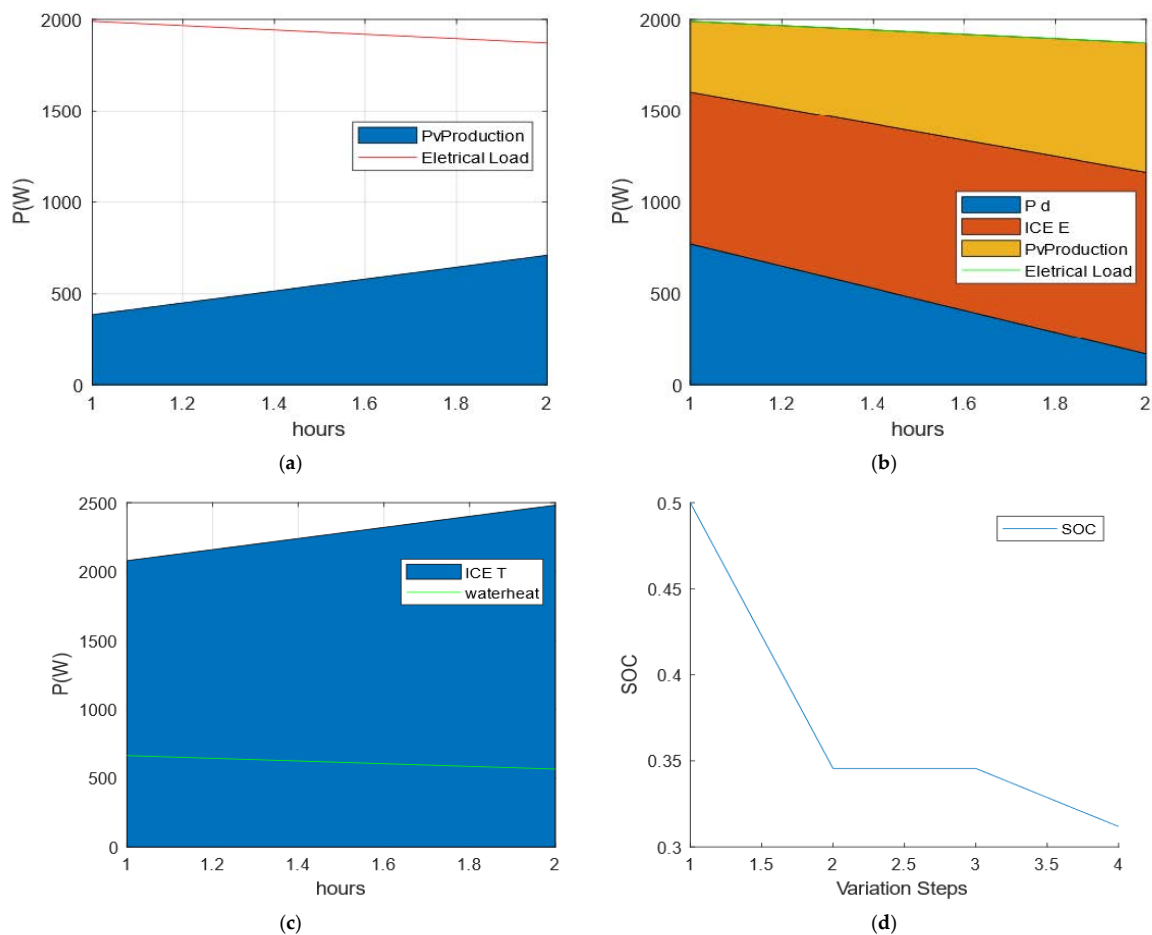


Figure 7. PV production deficit and SOC > 0.2: (a) demand of the electrical load and photovoltaic production; (b) electrical load profile; (c) water heating profile; (d) state of charge during the two prediction hours.

As depicted in Figure 7a,b, in the first forecasted hour, the PV generation deficit (with a forecasted electric demand of 1989 W and a PV power of 386 W) is offset by discharging 772 W from the battery. Because the battery cannot fully support the electrical load, 831 W of electrical power (ICE E) from the Micro-CHP compensates for the remainder. Moreover, 2079 W of thermal power (ICE T) from the Micro-CHP compensates for the 663 W water heating demand, with 1416 W of thermal surplus deployed for storage in a thermal accumulator.

During the second forecasted hour, 169 W from the battery and 992 W of electrical power (ICE E) from the Micro-CHP offsets the PV production deficit, given a forecasted electric demand of 1871 W and a PV power of 710 W. Considering the requirement to satisfy the water heating demand, the Micro-CHP system compensates with 2482 W of thermal power for the 565 W of demand. Here, 1917 W of thermal surplus is used for storage in a thermal accumulator. Figure 7d presents the SOC from the current time (SOC = 0.5) to the end of the two-hour forecast (SOC = 0.3). As described previously, in the first hour (1 to 2) the battery discharges to compensate for electrical demand, and in the second hour (3 to 4) the battery discharges to also compensate for demand.

At 1 pm on a sunny day, for peak demand and a scenario of excess PV production, where the SOC is less than 0.2, the results are shown in Figure 8.

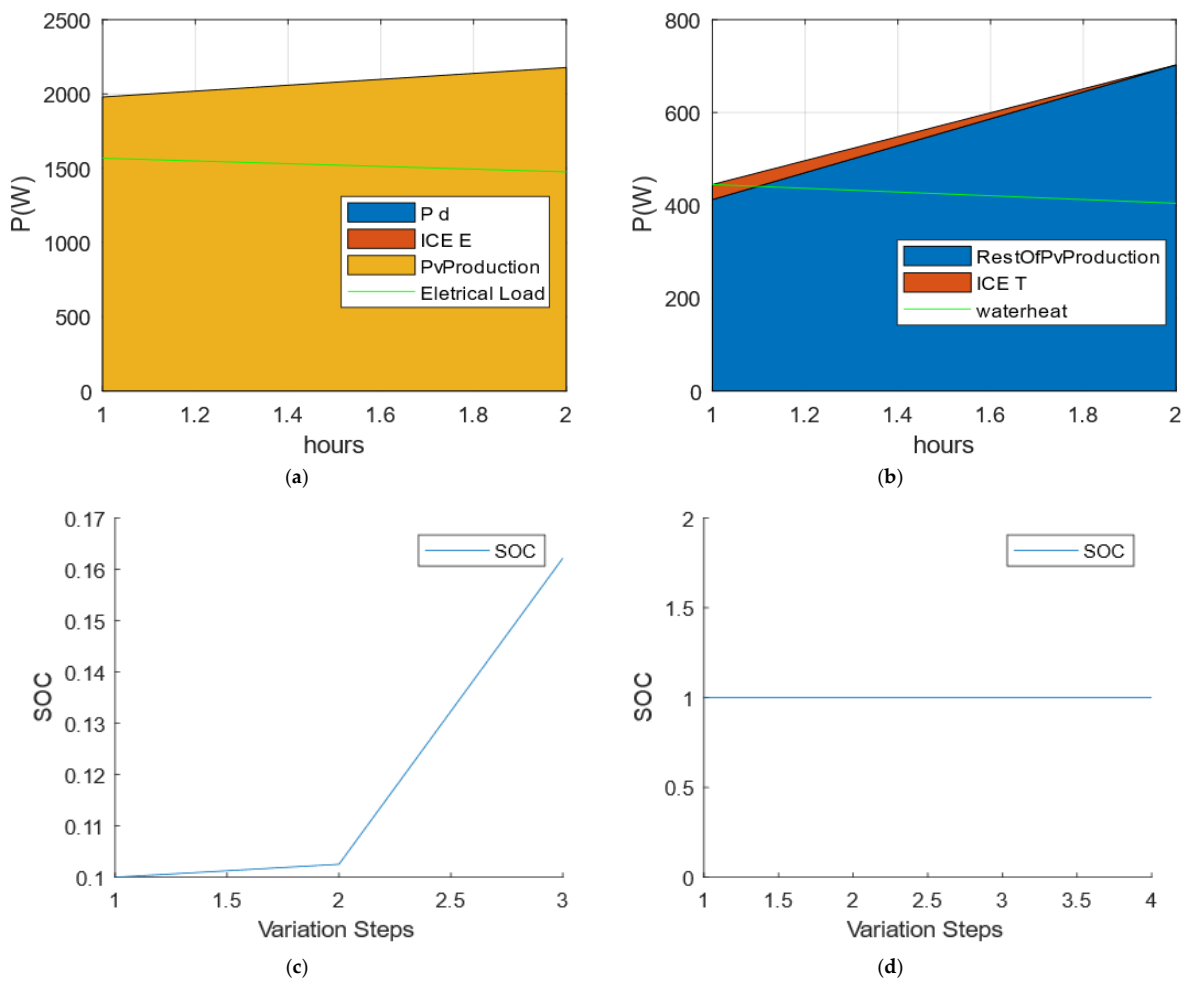


Figure 8. Excess PV production and SOC < 0.2: (a) electrical load profile; (b) water heating profile; (c) state of charge during the two prediction hours (initial SOC < 0.2); (d) state of charge during the two prediction hours (initial SOC = 1).

As observed in Figure 8a, during the first forecasted hour, where the photovoltaic power is 1980 W and the electrical demand is 1567 W, solar production fully covers the electrical demand. The excess PV production (412 W) assists in fulfilling the demand for water heating. However, since it does not entirely compensate, 32 W of thermal power from the Micro-CHP makes up the water heating demand (shown in Figure 8b). Additionally, 13 W of electrical power from the Micro-cogeneration system is used to charge the battery (1 to 2) (Figure 8c). In the second forecasted hour, with a photovoltaic power of 2178 W and an electrical demand of 1476 W, solar production completely satisfies the electrical demand.

The surplus solar production (702 W) caters to the water heating demand of 404 W. The remaining 298 W is used to charge the battery (as seen in Figure 8c).

For the situation of excess PV production and a SOC greater than 0.2, the results are identical to the previous case because there is no requirement to support the residential electrical demand with the battery. Consequently, the battery is charged in the same cycles (as shown in Figure 8c). In situations where the SOC equals 1 (shown in Figure 8d), it is not feasible to utilize the electrical energy from the Micro-CHP in the first prediction hour; 13 W is wasted because the battery is at its maximum SOC.

7.2. Simulation Setup and Scenarios (PV/Micro-CHP)

This simulation introduces a Micro-cogeneration system with electrical power ranging from 1.3 to 4.7 kW and thermal power from 4 to 12.5 kW into a residential grid, complemented by a photovoltaic (PV) panel with a power capacity of 3.5 kWp. In the situation of a PV production deficit, identical to the case examined in Section 7.1 (see Figure 6a), during the first forecasted hour, the PV generation deficit of 1603 W, arising from an expected electrical demand of 1989 W against a PV power of 386 W, is covered by the 1603 W electric power of the Micro-CHP system (as depicted in Figure 9a). The 663 W water heating demand is fulfilled by the 4009 W thermal power of the Micro-CHP, while the surplus of 3346 W of thermal power is allocated to storage in a thermal accumulator (Figure 9b). Similar operations are performed in the second forecast hour, with the 1161 W deficit being met by the Micro-CHP system’s electrical power (illustrated in Figure 9a). Additionally, 565 W of the water heating demand is compensated by the Micro-cogeneration system’s 2904 W thermal power, leaving a thermal surplus of 2339 W for storage in a thermal accumulator. In instances of excess PV production, following the same case simulated in Section 7.1 (shown in Figure 8a,b), the results remain consistent as anticipated.

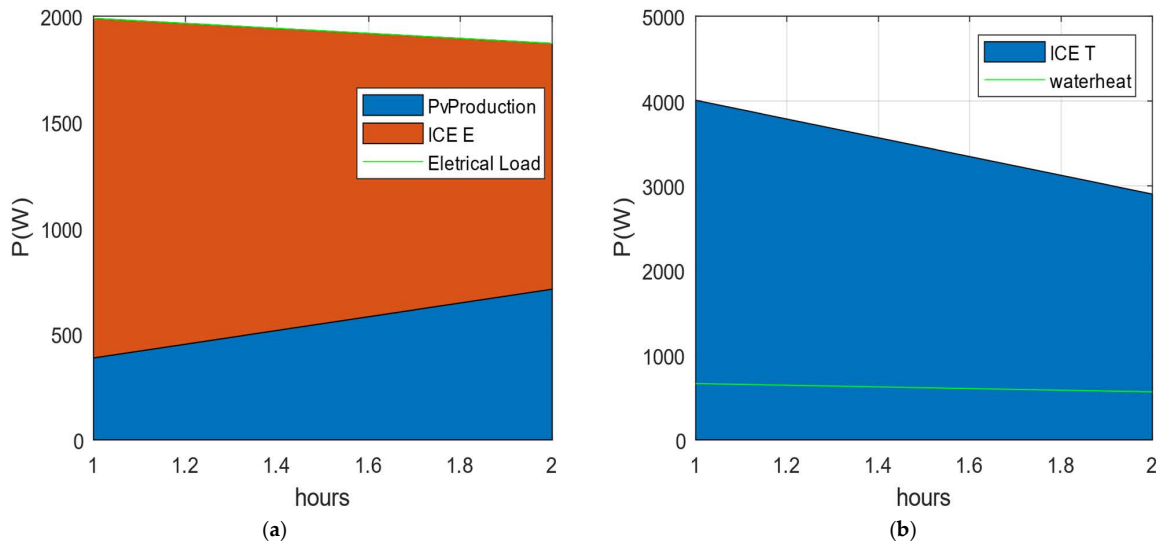


Figure 9. Deficit PV production: (a) electrical load profile; (b) water heating profile.

7.3. Simulation Setup and Scenarios (Battery/Micro-CHP)

The focus of this sub-section is the simulation of the interaction between the Micro-CHP and a battery within a residential network. The system incorporates a Micro-CHP unit with electrical power ranging from 1.3 to 4.7 kW and thermal power from 4 to 12.5 kW, alongside a battery with a capacity of 5 kWh. The scenario examined here is identical to the one represented in Figure 6a, with a battery state of charge (SOC) less than 0.2. The results are as follows: In the first hour of prediction, with an electrical load demand of 1989 W, the electric power of the Micro-CHP fully satisfies this demand (refer to Figure 10a). The 663 W water heating demand is met by 4974 W of thermal power of the Micro-CHP. The surplus 4311 W of thermal power is used for storage in a thermal accumulator (as

depicted in Figure 10b). Since the battery only supports the electrical load demand, the water heating demand is consistently covered by the thermal power of the Micro-CHP. Figure 10c provides a visual representation of the battery’s unitability.

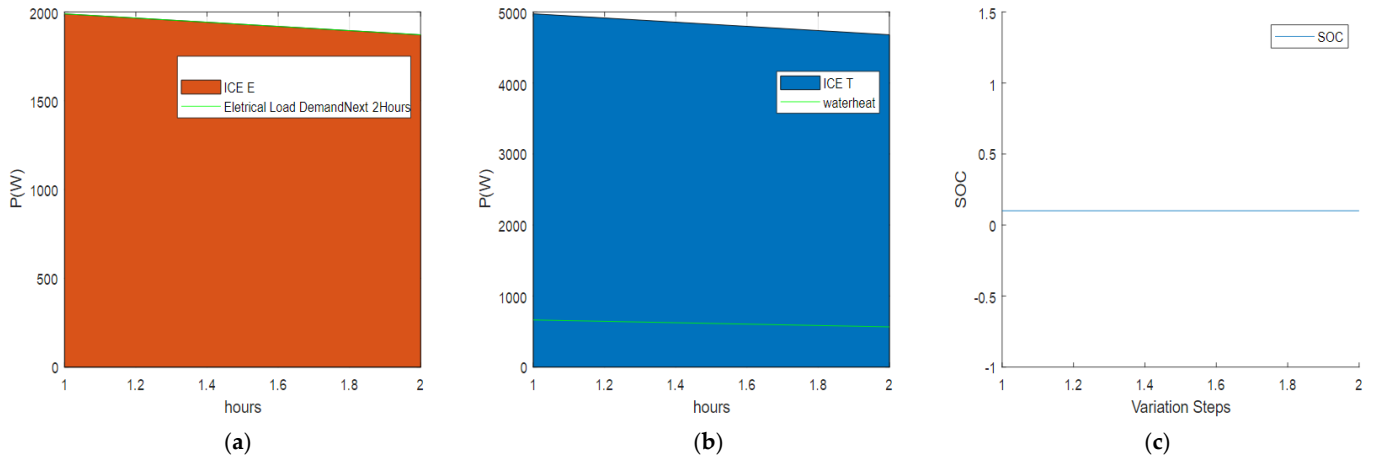


Figure 10. SOC < 0.2: (a) electrical load profile; (b) water heating profile; (c) state of charge during the two prediction hours.

In the second forecast hour, featuring an electrical load demand of 1871 W, the electric power of the Micro-CHP fully satisfies this demand. The water heating demand of 565 W is met by 4679 W of thermal power of the Micro-CHP, with the remaining 4114 W of thermal power utilized for storage in a thermal accumulator (refer to Figure 10b).

In cases where the state of charge (SOC) is greater than 0.2, the results unfold differently. In the first forecast hour, with a predicted electrical load demand of 1989 W, the battery supplies 772 W while the Micro-CHP compensates for the remaining load with 1217 W (refer to Figure 11a). The 663 W water heating demand is met by the 3044 W of thermal power of the Micro-CHP. The surplus of 2381 W of thermal power is used for storage in a thermal accumulator (as depicted in Figure 11b).

During the second forecasting hour, with an anticipated electrical load demand of 1871 W, the battery provides 169 W, and 1703 W is compensated by the electrical power from the Micro-CHP. The 565 W water heating demand is met by the 4258 W of thermal power of the Micro-CHP. The surplus 3693 W of thermal power is used for storage in a thermal accumulator (as depicted in Figure 11b).

As can be observed in Figure 11c, the battery discharges to support the load (1 to 4).

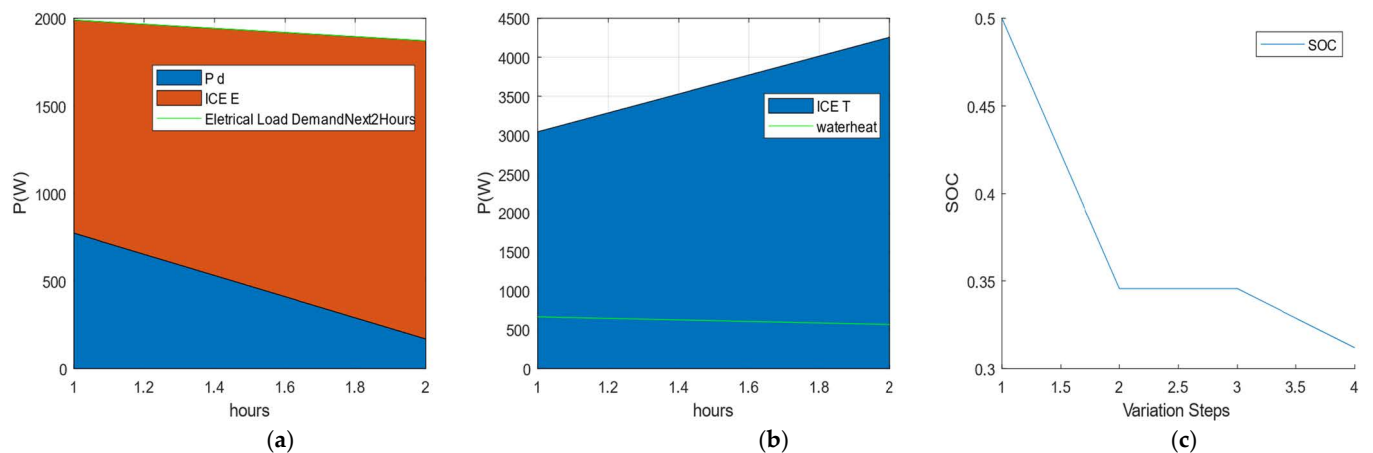


Figure 11. SOC > 0.2: (a) electrical load profile; (b) water heating profile; (c) state of charge during the two prediction hours.

8. Performance Evaluation of the Proposed Solution

Among the three system simulations performed, the PV/battery/Micro-CHP system demonstrated the highest profitability according to the findings. In the PV/Micro-CHP system, the load can be totally supported by the PV production; however, it falls short of completely satisfying the water heating demand, as indicated in Figure 8. This deficit makes it necessary to resort to the Micro-CHP system. Ideally, in this scenario, the electrical energy should be directed to battery charging. But in the absence of a means of storage, a waste of 13 W is inevitable. However, this waste does not have a significant impact on the overall profitability of the system since photovoltaic production covers 98% of electricity demand and water heating needs.

In conditions where photovoltaic production is deficient, the energy generated by the engine matches the output of the battery/Micro-CHP system. However, the former is more efficient due to its partial reliance on renewable energy sources. In the battery/Micro-CHP system, the primary technology supporting the water heating demand is the Micro-CHP, making the system heavily dependent on it. The inclusion of a battery helps to minimize the electric and thermal power production when the Micro-CHP and the battery jointly support the electricity demand, thanks to the ability of the system to vary the electric and thermal production. Power losses only occur if the state of charge (SOC) is at maximum capacity, as energy is then diverted to meet residential electrical demand or charged to the battery.

Comparing the use of the cogeneration system with the conventional system, the Micro-CHP is more efficient in water heat demand in addition to solving the need for electricity production. Considering the thermal efficiency mentioned above for the Micro-CHP and electrical efficiency, from the conventional use of an electric storage water heater (ESWH) of 40%, the results of the power required to satisfy 663 W of water heat demand are as shown in Figure 12.

To reach 663 W of water heating demand, in the first hour of the profile of Figure 5c, it is necessary to introduce 1657 W of electric power in the system without the Micro-CHP (2); a little bit higher in value compared to the system with the Micro-CHP (1) that needs 1033 W. It is confirmed that the conventional use of an ESWH is less efficient compared to the use of a system with the Micro-CHP.

Figure 12 compares the same case, but instead of an ESWH, if the comparison is made with a heat pump (that nowadays can reach 111% efficiency) to reach 663 W of water heating demand, in the first hour of the profile of Figure 5c, it is necessary to introduce 597 W of electrical power in the system with the heat pump (2). The value is lower, compared to the system with the Micro-CHP (1), which needs 1033 W. Considering the case study, there is a higher efficiency for the Micro-CHP to satisfy the water heating demand. Despite the reduced efficiency compared to the heat pump, with the Micro-CHP, the system becomes more autonomous because, besides the thermal energy production, electric energy is produced in the same process allowing better management of the system, unlike heat pumps which do not add anything to the electricity grid. This electrical energy can be directed to the battery in case the PV power does not fully compensate for the water heating demand, as is visible in the case of Figure 8b,c. On the other hand, it can compensate for the household electric demand when the battery SOC is reduced, as is the case in Figure 6b.

Continuous enhancements and adjustments were integrated throughout the study to enhance the overall efficiency, resilience, and autonomy of the grid. The use of a Micro-CHP system with adjustable output avoids the need for a constant output at different load profiles. This flexibility avoids wasted energy and allows the Micro-CHP system to adapt to the required demand. Significant emphasis was placed on establishing priority assumptions from the outset, such as supporting an electric load and subsequently meeting the demand for water heating from thermal energy storage; more specifically, an electric water cylinder.

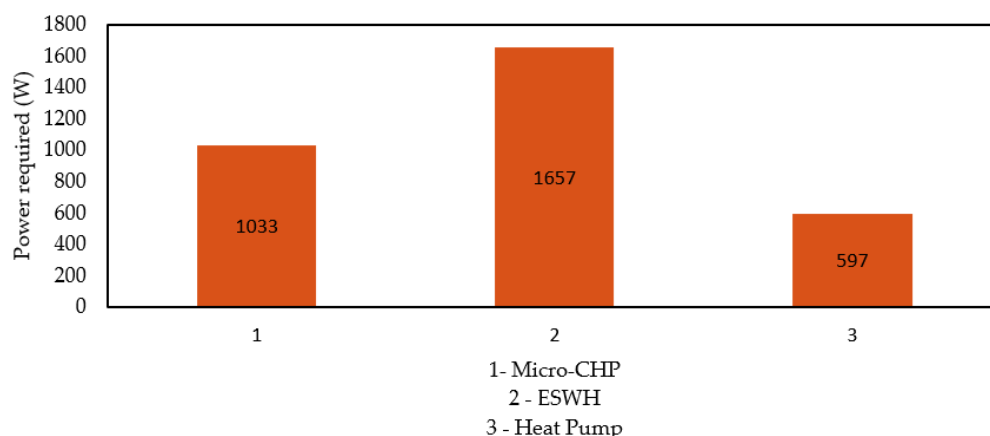


Figure 12. Comparing the power required to compensate 663 W of water heating demand of the Micro-CHP, an ESWH, and a heat pump.

9. Conclusions

9.1. Summary of Findings

The development of an electrical load and photovoltaic (PV) production forecasting tool based on a feedforward neural network (FFNN) was a significant step toward enhancing energy management in this study. This tool allowed for optimal operational planning over a two-hour horizon, ensuring that the output of the Micro-combined heat and power (Micro-CHP) system was meticulously managed to minimize energy wastage.

The forecasting tool proved instrumental in pre-emptively driving the engine operation, enabling the system to strategically modulate the electrical or thermal output to align with the anticipated demand conditions. The anticipation of changes in load allowed for the optimal use of the Micro-CHP system's output, contributing significantly to the improvement of the system's efficiency and the overall reduction in energy wastage.

When the Micro-CHP was integrated into a PV/battery/Micro-CHP system, the gains were most substantial. The interplay between the Micro-CHP, battery, and PV production allowed for a highly efficient and reliable energy system, ensuring that demand could be met under various conditions while reducing dependency on the grid. Comparatively, the system incurred negligible losses in comparison to the standalone PV/Micro-CHP system, demonstrating the benefit of integrating a battery into the energy system.

On the other hand, in the battery/Micro-CHP system configuration, expenses were slightly higher, as the Micro-CHP served as the core component of the system. It was responsible for catering to a significant proportion of the demand and was, therefore, subject to more extensive use, which resulted in higher operational costs.

However, the study revealed that the optimal system configuration was achieved when the Micro-CHP was utilized as a backup energy source. In this configuration, the Micro-CHP system could step in to supply the required load in instances of a photovoltaic deficit or when the state of charge (SOC) of the battery fell below 0.2. This setup ensured that the system could function entirely off-grid during these periods, thereby contributing to significant improvements in system efficiency while enhancing grid independence and resilience.

9.2. Contributions to Grid Resilience, Energy Efficiency, and Renewable Energy Integration

The findings and methodologies presented in this research make a significant contribution to enhancing grid resilience, energy efficiency, and the incorporation of renewable energy. The optimization of the PV, battery, and Micro-CHP systems in a single platform ensures that not only is the supply of energy consistent, even during instances of photovoltaic deficits, but also that energy usage is optimized, effectively minimizing wastage.

The effective management of the proposed model serves to greatly improve the resilience of residential grids by integrating a robust and efficient backup system. This

backup system, powered by the Micro-CHP unit, ensures that a reliable and steady source of power is always available to meet demand, even in situations where renewable energy sources are inadequate. This effectively strengthens the ability of the grid to withstand and adapt to changing conditions, significantly enhancing its overall resilience.

In terms of energy efficiency, this research's model takes significant strides forward. The meticulous planning and operational control allowed by the forecasting tool ensure that the Micro-CHP system's output is optimally used, minimizing energy wastage and thereby improving overall energy efficiency. This improved efficiency not only reduces operational costs but also contributes to the overall sustainability of the system.

Furthermore, this study contributes meaningfully to the broader push toward renewable energy integration. The proposed model harnesses the power of renewable energy sources, namely photovoltaic panels, to meet residential demand for electricity and hot water. By developing a system that can operate independently of the grid during periods of low battery state of charge and photovoltaic deficits, this research facilitates increased utilization and adaptability of renewable energy resources. This not only reduces dependency on conventional, non-renewable energy sources but also helps propel the move towards a more sustainable, renewable energy future.

By efficiently combining renewable sources and storage with a backup Micro-CHP system, the proposed model allows for a more flexible and sustainable energy supply. It marks a step forward in the direction of creating more resilient, efficient, and sustainable energy systems, effectively addressing some of the most pressing challenges of our current energy landscape.

9.3. Limitations and Future Work

While this study has yielded promising results and insights, it is essential to acknowledge that the current literature on the integration of a Micro-CHP into a PV/battery/Micro-CHP system is sparse. There is considerable potential for such integrated systems in various settings, especially in buildings and residential complexes. The development and implementation of off-grid systems like the one proposed in this study can greatly enhance the interconnectivity between residential demands and surrounding technologies, ultimately offering comprehensive benefits across multiple aspects of energy use and management.

However, even with the notable advances presented in this research, there remain areas for further exploration and improvement. One such area is the more effective utilization of thermal power. Despite the optimization measures put in place, thermal power still constitutes the most wasted part of the system, indicating a substantial opportunity for further enhancements in system efficiency.

As a prospective avenue for future research, it is worth considering the development of thermal energy storage systems. Such systems could effectively store energy to be utilized for various thermal applications, providing heat when needed. This approach would not only enhance the efficient utilization of thermal power but also lead to overall improvements in system performance. Exploring and implementing thermal energy storage solutions holds great potential for advancing the effectiveness and efficiency of the system, thereby contributing to its overall performance enhancements.

Additionally, future research could delve into optimizing the system across diverse weather conditions and geographical locations, recognizing the significant influence these factors have on PV production and the requirements for residential temperature management. Such work could help to make the system even more versatile and adaptable, enhancing its suitability for a broader range of applications.

In conclusion, while this study marks a significant step forward in the optimization of Micro-cogeneration systems within residential grids, there remains much potential for further research and development. It is anticipated that the continuation of work in this area will yield even more efficient, flexible, and sustainable solutions for residential energy management.

Author Contributions: Conceptualization, D.C. and D.N.; methodology, D.C. and D.N.; software, D.N. and D.C.; validation, P.F. and P.D.G.; formal analysis, P.F. and P.D.G.; investigation, D.C., D.N. and P.F.; data curation, J.F.; writing—original draft preparation, D.C. and D.N.; writing—review and editing, D.C., D.N., P.F. and P.D.G.; supervision, P.F. and P.D.G. All authors have read and agreed to the published version of the manuscript.

Funding: The authors would like to express their gratitude to Fundação para a Ciência e Tecnologia (FCT) and C-MAST (Centre for Mechanical and Aerospace Science and Technologies) for their support in the form of funding under the project UIDB/00151/2020.

Conflicts of Interest: The authors declare no conflict of interest.

References

1. Faria, J.; Pombo, J.; Mariano, S.; Rosario Calado, M.D. Power Management Strategy for Standalone PV Applications with Hybrid Energy Storage System. In Proceedings of the 2018 IEEE International Conference on Environment and Electrical Engineering and 2018 IEEE Industrial and Commercial Power Systems Europe (EEEIC/I&CPS Europe), Palermo, Italy, 12–15 June 2018; Volume 1–6, p. 101109.
2. Entchev, E.; Yang, L.; Ghorab, M.; Rosato, A.; Sibilio, S. Energy, economic and environmental performance simulation of a hybrid renewable Microgeneration system with neural network predictive control. *Alex. Eng. J.* **2018**, *57*, 455–473. [[CrossRef](#)]
3. Ribberink, H.; Entchev, E. Exploring the potential synergy between Micro-cogeneration and electric vehicle charging. *Appl. Therm. Eng.* **2014**, *71*, 677–685. [[CrossRef](#)]
4. Koohi-Fayegh, S.; Rosen, M.A. A review of energy storage types, applications, and recent developments. *J. Energy Storage* **2020**, *27*, 101047. [[CrossRef](#)]
5. Kang, E.-C.; Lee, E.-J.; Ghorab, M.; Yang, L.; Entchev, E.; Lee, K.-S.; Lyu, N.-J. Investigation of energy and environmental potentials of a renewable trigeneration system in a residential application. *Energies* **2016**, *9*, 760. [[CrossRef](#)]
6. Mikalsen, R. Internal combustion and reciprocating engine systems for small and Micro combined heat and power (CHP) applications. In *Small and Micro Combined Heat and Power (CHP) Systems*; Elsevier: Amsterdam, The Netherlands, 2011; Volume 125–146, p. 101533.
7. Frangopoulos, C.A. *EDUCOGEN, The European Educational Tools on Cogeneration*; European Commission: Brussels, Belgium, 2001.
8. Onovwiona, H.I.; Ugursal, V.I. Residential cogeneration systems: Review of the current technology. *Renew. Sustain. Energy Rev.* **2006**, *105*, 389–431. [[CrossRef](#)]
9. Orlando, J.A. *Cogeneration Design Guide*; ASHRAE: Atlanta, GA, USA, 1996.
10. Chicco, G.; Mancarella, P. Assessment of the greenhouse gas emissions from cogeneration and trigeneration systems. Part I: Models and indicators. *Energy* **2008**, *33*, 410–417. [[CrossRef](#)]
11. Tanaka, H.; Suzuki, A.; Yamamoto, K.; Yamamoto, I.; Yoshimura, M.; Togawa, K. New Ecowill—A new generation gas engine Micro-CHP. In Proceedings of the International Gas Union Research Conference 2011, Seoul, Republic of Korea, 19–21 October 2011.
12. Japan's Smallest Gas Engine Cogeneration System. The Netherlands: Centre for the Analysis and Dissemination of Demonstrated Energy Technologies. In *CADDET Energy Efficiency*; IEA/OECD: Paris, France, 2001.
13. Alcaide, F.; Cabot, P.-L.; Brillas, E. Fuel cells for chemicals and energy cogeneration. *J. Power Sources* **2006**, *153*, 47–60. [[CrossRef](#)]
14. Milcarek, R.J.; Ahn, J.; Zhang, J. Review and analysis of fuel cell-based, Micro-cogeneration for residential applications: Current state and future opportunities. *Sci. Technol. Built Environ.* **2018**, *23*, 1224–1243. [[CrossRef](#)]
15. Little, A.D. Volume I: Main Text. In *Opportunities for Micropower and Fuel Cell/Gas Turbine Hybrid Systems in Industrial Applications*; Arthur D. Little, Inc.: Cambridge, MA, USA, 2000; Volume 1, p. 173.
16. Isa, N.M.; Tan, C.W.; Yatim, A.H.M. A comprehensive review of cogeneration system in a Microgrid: A perspective from architecture and operating system. *Renew. Sustain. Energy Rev.* **2018**, *81*, 2236–2263. [[CrossRef](#)]
17. Darcovich, K.; Henquin, E.R.; Kenney, B.; Davidson, I.J.; Saldanha, N.; Beausoleil-Morrison, I. Higher-capacity lithium ion battery chemistries for improved residential energy storage with Micro-cogeneration. *Appl. Energy* **2013**, *111*, 853–861. [[CrossRef](#)]
18. Desideri, U.; Cinti, G.; Discepoli, G.; Sisani, E.; Penchini, D. SOFC Micro-CHP integration in residential buildings. In *Proceedings of the 25th International Conference on Efficiency, Cost, Optimization and Simulation of Energy Conversion Systems and Processes, ECOS 2012*; Firenze University Press: Firenze, Italy, 2012; pp. 26–29.
19. Quaschnig, V. *Understanding Renewable Energy Systems*; Routledge: Abingdon, UK, 2016.
20. Faizollahzadeh Ardabili, S.; Mahmoudi, A.; Mesri Gundoshmian, T. Modeling and simulation controlling system of HVAC using fuzzy and predictive (radial basis function, RBF) controllers. *J. Build. Eng.* **2016**, *6*, 301–308. [[CrossRef](#)]
21. Karballaezadeh, N.; Mohammadzadeh, S.D.; Shamshirband, S.; Hajikhodaverdikhan, P.; Mosavi, A.; Chau, K.W. Prediction of remaining service life of pavement using an optimized support vector machine. *Eng. Appl. Comput. Fluid Mech.* **2019**, *13*, 188–198.
22. Faizollahzadeh Ardabili, S.; Najafi, B.; Shamshirband, S.; Minaei Bidgoli, B.; Deo, R.C.; Chau, K.-W. Computational intelligence approach for modeling hydrogen production: A review. *Eng. Appl. Comput. Fluid Mech.* **2018**, *12*, 438–458. [[CrossRef](#)]
23. Mosavi, A.; Salimi, M.; Faizollahzadeh Ardabili, S.; Rabczuk, T.; Shamshirband, S.; Varkonyi-Koczy, A. State of the Art of Machine Learning Models in Energy Systems, a Systematic Review. *Energies* **2019**, *12*, 1301. [[CrossRef](#)]

24. Zhang, J.; Walter, G.G.; Miao, Y.; Lee, W.N.W. Wavelet neural networks for function learning. *IEEE Trans. Signal Process.* **1995**, *43*, 1485–1497. [[CrossRef](#)]
25. Faizollahzadeh Ardabili, S.; Najafi, B.; Ghaebi, H.; Shamsirband, S.; Mostafaeipour, A. A novel enhanced exergy method in analyzing HVAC system using soft computing approaches: A case study on mushroom growing hall. *J. Build. Eng.* **2017**, *13*, 309–318. [[CrossRef](#)]
26. Mandelli, S.; Brivio, C.; Colombo, E.; Merlo, M. A sizing methodology based on Levelized Cost of Supplied and Lost Energy for off-grid rural electrification systems. *Renew. Energy* **2016**, *89*, 475–488. [[CrossRef](#)]
27. Okoye, C.O.; Solyali, O. Optimal sizing of stand-alone photovoltaic systems in residential buildings. *Energy* **2017**, *126*, 573–584. [[CrossRef](#)]
28. Zhang, Q.; Li, Y.; Shang, Y.; Duan, B.; Cui, N.; Zhang, C. A Fractional-Order Kinetic Battery Model of Lithium-Ion Batteries Considering a Nonlinear Capacity. *Electronics* **2019**, *8*, 394. [[CrossRef](#)]
29. Rodrigues, L.; Montez, C.; Moraes, R.; Portugal, P.; Vasques, F. A Temperature-Dependent Battery Model for Wireless Sensor Networks. *Sensors* **2017**, *17*, 422. [[CrossRef](#)] [[PubMed](#)]
30. Manwell, J.F.; McGowan, J.G. Lead acid battery storage model for hybrid energy systems. *Solar Energy* **1993**, *50*, 399–405. [[CrossRef](#)]
31. Amarasinghe, K.; Marino, D.L.; Manic, M. Deep neural networks for energy load forecasting. In Proceedings of the 2017 IEEE 26th International Symposium on Industrial Electronics (ISIE), Edinburgh, UK, 19–21 June 2017; pp. 1483–1488.
32. Zhang, H.-T.; Xu, F.-Y.; Zhou, L. Artificial neural network for load forecasting in smart grid. In Proceedings of the 2010 International Conference on Machine Learning and Cybernetics, Qingdao, China, 11–14 July 2010; pp. 3200–3205.
33. Lai, L.L.; Subasinghe, H.; Rajkumar, N.; Vaseekar, E.; Gwyn, B.J.; Sood, V.K. Object-oriented genetic algorithm based artificial neural network for load forecasting. In Proceedings of the Simulated Evolution and Learning: Second Asia-Pacific Conference on Simulated Evolution and Learning, SEAL'98, Canberra, Australia, 24–27 November 1999; pp. 462–469.
34. Bento, P.M.R.; Pombo, J.A.N.; Calado, M.R.A.; Mariano, S.J.P.S. Optimization of neural network with wavelet transform and improved data selection using bat algorithm for short-term load forecasting. *Neurocomputing* **2019**, *358*, 53–71. [[CrossRef](#)]
35. Islam, B.U. Comparison of conventional and modern load forecasting techniques based on artificial intelligence and expert systems. *Int. J. Comput. Sci. Issues* **2011**, *8*, 504–513.

Disclaimer/Publisher's Note: The statements, opinions and data contained in all publications are solely those of the individual author(s) and contributor(s) and not of MDPI and/or the editor(s). MDPI and/or the editor(s) disclaim responsibility for any injury to people or property resulting from any ideas, methods, instructions or products referred to in the content.